GEOLOGICA CARPATHICA, AUGUST 2009, 60, 4, 295–305 doi: 10.2478/v10096-009-0021-4

Markov Chain analysis of turbiditic facies and flow dynamics (Magura Zone, Outer Western Carpathians, NW Slovakia)

SIDÓNIA STAŇOVÁ, JÁN SOTÁK and NORBERT HUDEC

Geological Institute of the Slovak Academy of Sciences, Severná 5, 974 01 Banská Bystrica, Slovak Republic;
stanova@savbb.sk; sotak@savbb.sk

(Manuscript received April 17, 2008; accepted in revised form December 18, 2008)

Abstract: Methods based on the Markov Chains can be easily applied in the evaluation of order in sedimentary sequences. In this contribution Markov Chain analysis was applied to analysis of turbiditic formation of the Outer Western Carpathians in NW Slovakia, although it also has broader utilization in the interpretation of sedimentary sequences from other depositional environments. Non-random facies transitions were determined in the investigated strata and compared to the standard deep-water facies models to provide statistical evidence for the sedimentological interpretation of depositional processes. As a result, six genetic facies types, interpreted in terms of depositional processes, were identified. They comprise deposits of density flows, turbidity flows, suspension fallout as well as units which resulted from syn- or post-depositional deformation.

Key words: Outer Western Carpathians, facies, density flows, Markov Chains, turbidite.

Introduction

Sedimentologists in their field work usually provide records of sedimentary rocks. One of the routine ways to make a sedimentary record is to plot the studied sedimentary rocks as a vertical section of successive facies. Sediment facies represent sediment or sedimentary rock that display distinctive physical, chemical and/or biological characteristics (Stow 2005). There are descriptive and genetic facies. While descriptive facies are defined purely on sedimentary characteristics, such as muddy sandstone, laminated mudstone, etc., genetic facies are determined by the comparison with standard facies models and interpreted in terms of depositional processes, such as turbidite, contourite, lahar deposit, etc. The key to the interpretation of the sedimentary record is to study facies in association, in particular their relative vertical and lateral positions (Graham 1988). Comparison of descriptive facies from the study area with standard facies models for different depositional systems is a useful practice (Stow 2005). However, the balance of data being interpreted against models tempts us to look for some kind of arrangement, even if there is no order (Carr 1982). Application of statistical techniques provides an opportunity to the reduce subjective impact on interpretations of the sedimentological record. Some simple statistical methods have been applied to detect the possible presence of vertical order in sedimentary successions. Almost all use the probability matrices and employ the idea of Markov Chains. In this study, the Markov property was applied to validate the presence of order in the sequence of structures or descriptive facies in the turbiditic formation from the Outer Western Carpathians. The main goal of this study was to find statistically significant successions of descriptive facies in the investigated strata and compare them to the facies models of deep-water deposits with the purpose of supporting sedimentological interpretations of depositional processes. The Markov Chain analysis has commonly been used in the past for the analysis of ordered sequences from a wide range of depositional environments. However, the calculations in the analysis of ordered succession of facies with the assistance of the Markov Chains are time consuming. As a consequence, a simple computer program entitled "phpSedistat" was devised for this study to make the calculations easier.

General approach

A Markov process describes a sequence of states, or events, for which the occurrence of one state may exhibit a dependence on a previous state or states (Powers & Easterling 1982). Development of methods based on the Markov property which can be used in geology started at the end of the 60's. They have been used by a number of investigators (e.g. Potter & Blakey 1968; Gingerinch 1969; Read 1969; Doveton 1971; Miall 1973; Ethier 1975) to validate the presence of ordered and cyclic successions of facies. Stratigraphic "order" may be indicated by repeated patterns of either thickness and/or lithological variation, but it should also be noted that the presence of lithological order alone makes no compelling argument for periodic accumulation (Wilkinson et al. 1997). On that account, the Markov property proved to be of little use for characterizing sedimentary cyclicity (Weedon 2005). However, it was considered useful, when for example, the particular order of lithologies helps in the description of sedimentological processes (Wilkinson et al. 1997). This is why the Markov property has been used in this study, which is focused on the analysis of facies and flow dynamics of turbiditic formation.

The presence of Markov process implies a degree of order in a system (Carr 1982). In most studies, the raw data consist

of an observed number of upward facies transitions which are plotted in matrix form (transition matrix) and compared to one generated by random methods (Graham 1988). The initial works in this field proceeded from a mistaken mathematical technique of generating an independent trial matrix and resulted in inappropriate conlusions. The transition matrix can be determined in two ways (Powers & Easterling 1982). One method is to make observations at regular intervals of thickness. The advantage of this method is that the diagonal frequencies of the transitional matrix carry information about thickness, but a disadvantage is that observed transition rates depend on the sampling interval. An alternative method is to construct a sequence of lithologies by recording the transitions of lithologies as they occur, withouth regard to thickness. Since the transition from a bed of one lithology (facies) to another case of the same type is assumed to be objectively non-recordable, the diagonal frequencies are constrained zero. Transition matrices containing structural zeroes are called embedded matrices. Then observed facies transitions are compared to wholly random facies transitions. It was pointed out by Schwarzacher (1975) that the presence of previously defined zeroes was a major obstacle for accurate analysis (Graham 1988). Attempting to overcome this problem, both Carr (1982) and Powers & Easterling (1982) independently recommended a method (effectively the same one) for the estimation of wholly random facies transitions, termed quasi-independence, by employing a technique initially developed by Goodman (1968). The expected transition frequencies under a model of quasi-independence are generated by an iterative method (Powers & Easterling 1982). In the identification of significant transitions, the observed and expected cells are used to derive a difference matrix (Gingerich 1969; Carr 1982). The positive values in the difference matrix were regarded as non-random, while negative values were regarded as random, which led to some questionable conclusions in initial works. Consequently it has been suggested that all positive values in the difference matrix have to be statistically tested for randomness (Harper 1984).

Geological settings

The research area extends in the NW, Slovak part of the Outer Western Carpathians (Fig. 1), contouring the northerly convex arcuate shape of the Western Carpathian orocline. The Western Carpathians create the northernmost, W-E trending orocline of the European Alpides, linked through the Vienna Basin to the Eastern Alps in the West and to the Eastern Carpathians in the East (Plašienka et al. 1997). The present structural pattern of the Western Carpathians was formed by the Late Jurassic-Tertiary subduction-collision orogenic processes in the Tethyan mobile belt between the stable North European Platform and drifting Apulia/Adria related continental fragments. The Outer Western Carpathians contain sediments of the late Tertiary Carpathian Foredeep deposited on the southern flanks of the North European Platform and a broad Flysch Belt. Several thousands of meters thick Upper Jurassic to Lower Miocene, mostly siliciclastic, flysch deposits built up several nappes, subhorizontally overthrusted onto Miocene deposits of the Carpathian Foredeep or directly onto Precambrian, Paleozoic or Mesozoic rocks of the Carpathian foreland (Oszczypko et al. 2003). They are completely uprooted from their basement and separated from the Central Carpathians by the Pieniny Klippen Belt suture zone. Little is known about the nature of the Flysch Belt basement substratum which was shortened and underthrust below the Central Western Carpathians during the Tertiary (Plašienka et al. 1997).

The Flysch Belt represents the Tertiary accretionary wedge of the Carpathian orogen. The flysch nappes are generally arranged into the Silesian–Moldavian (or "Krosno-Menilite") group of nappes in the North, and the Magura thrust system in the South (Plašienka et al. 1997). In the research area, there are several large thrust units of the Magura Group, consisting of the Rača, Bystrica and Oravská Magura (Krynica) Units.

All the studied sedimentary sections expose the Kýčera Member of Rača Unit, deposited in the Magura Basin during the Late Eocene. On the basis of the field sedimentary research, the Kýčera Member represents a sandstone-dominated sequence alternating with mudstone rich intervals. The sandstones mostly form thin to thick beds, although some very thick beds are present as well. Most sandstone beds have parallel or slightly wavy bases. Amalgamation of beds is common. It is sometimes indicated by clustered amalgamation clasts (Fig. 2D). Generally, mud clasts float in the upper part of a bed (Fig. 2H,J). Medium to very thick beds of structureless sandstones and pebbly sandstones with normal gradation of pebbles are present. A lot of them have T_{b-d} Bouma divisions in the upper part of beds (Fig. 2A,B) or most frequently they have only a thin laminated mudstone top directly above T_a Bouma interval. These thin laminated tops are often bioturbated (Fig. 2C). The upper parts of sandstone beds are frequently eroded by the next current or reworked by bottom currents. Mudstone rich intervals contain thick claystones/silty claystones or thick beds of claystone/silty claystone with mm to cm silt/very fine sandstone laminae (Fig. 2K). The Kýčera Member represents either channel systems (or upper parts of lobes) alternating with interchannel areas (Starek & Pivko 2001) or depositional lobes alternating with interlobe deposits (Staňová & Soták 2007). The Kýčera Member belongs to the Zlín Formation, which terminated the deposition in the Rača Unit. The Kýčera Member is considered equivalent to the muscovite sandstone facies of the "Magura Sandstone" of the Polish Western Carpathians (Ksiazkiewicz 1953; Pivko 2002).

Methodology

Detailed field sedimentary research was carried out in a series of quarries and road-cut exposures in the NW Slovak part of the Magura Group of the Outer Western Carpathians (Figs. 1, 2). In the field research extended attention was given to detailed study of sedimentary structures. Visual comparators were used in the field to determine grain sizes. The starting point for data analysis and interpretation is the vertical section of sedimentary sequence. The main members of

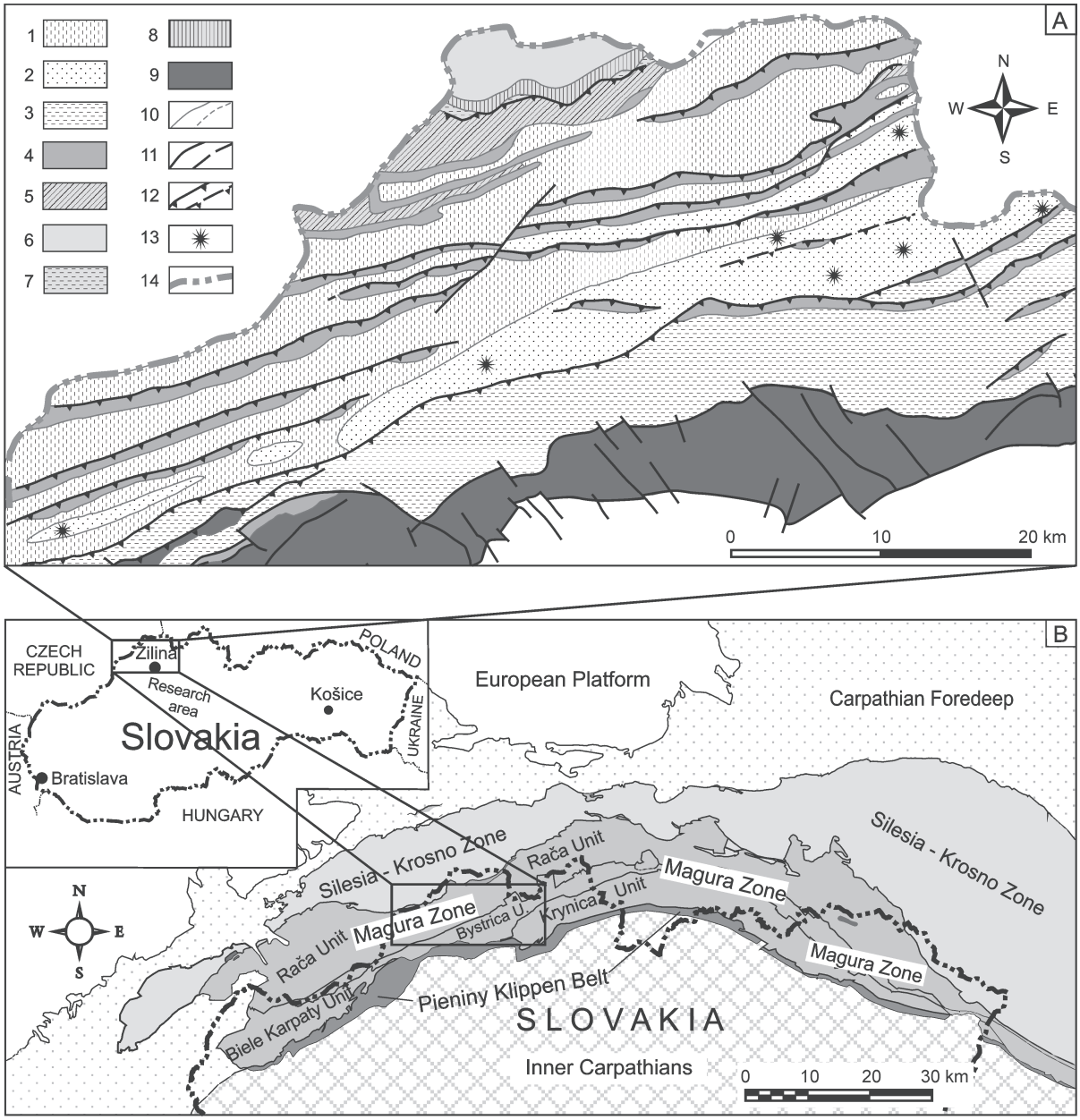

Fig. 1. A — Geological map of investigated area showing the locations of the outcrops of the Kýčera Member. **1–5** — Magura Group: 1 — Vsetín Member, 2 — Kýčera Member, Babia Góra Sandstone, 3 — Bystrica Member, 4 — Beloveža Formation ("Variegated beds"), 5 — Soláň Formation; **6–8** — Silesia Group: 6 — Istebná Member, 7 — Krosno Formation, 8 — Hieroglyph Formation; **9** — Pieniny Klippen Belt; **10** — geological boundaries: determined, expected; **11** — fractures: determined, expected; **12** — lines of the nappes and thrusts: determined, expected; **13** — localities; **14** — state boundary (modified from Biely et al. 1996). **B** — Location of the research area on the tectonic scheme of the Outer Western Carpathians (modified from Żytko K. et al. in Poprawa & Nemčok 1989).

sedimentary sequences — descriptive facies were defined on the basis of sedimentary characteristics recorded in the field and marked with facies codes.

The presence of order in the studied successions of facies was validated using the statistical methods based on the Markov property. The procedures for the calculation of significant facies transitions were incorporated into a self-designed computer program, entitled "phpSedistat", allowing automation of the calculations (see Appendix for details). As the calculations are practically provided using a computer program, attention is given to the input data for calculation and to the form and interpretation of the output data. The input data for the calculation is a vertical sequence of facies, expressed as a column of facies codes representing descriptive facies and saved in a .txt file. Interruptions or absence of sedimentary record is marked with a dividing symbol (*/*).

The output data are: (1) a list of facies codes and short description of associated facies, (2) a matrix of observed facies transitions and (3) a matrix of significant facies transitions. The matrix of observed facies transitions contain the number

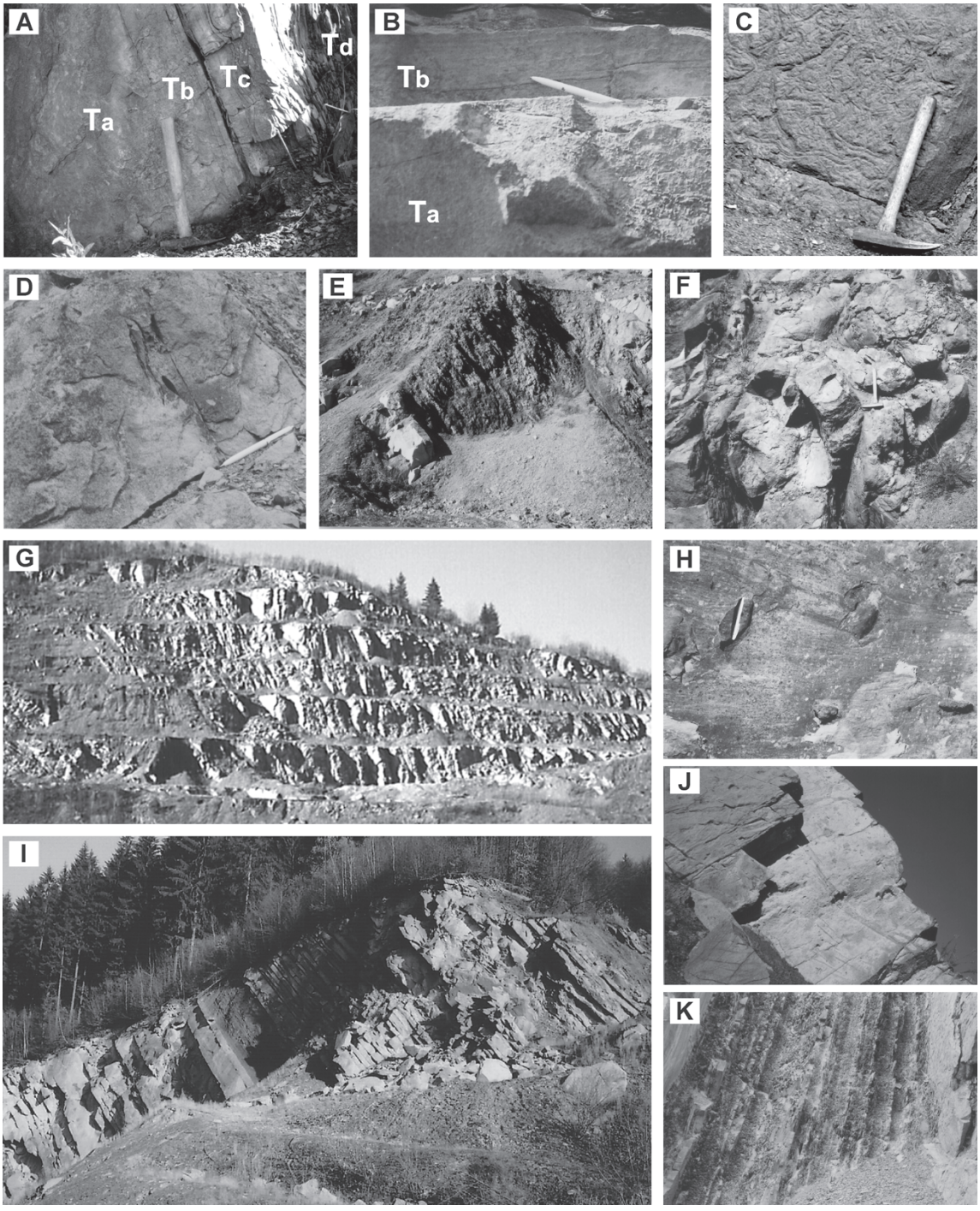

Fig. 2. Photographs showing some general views and structures of investigated outcrops of the Kýčera Member. See the outcrop locations on Fig. 1A. **A** — Detailed view from Krásno nad Kysucou outcrop showing the turbidite deposit, described by the Bouma model, consisting of massive sandstone, T_a at the base passing to the lower parallel lamination, T_b, wave lamination, T_c and upper parallel lamination, T_d at the top. **B** — Detailed view from the outcrop in Lysá pod Makytou quarry showing massive sandstone followed by laminated sandstone (T_{ab} Bouma sequence). **C** — Field photograph of *Taphrhelminthopsis* traces in laminated siltstones on the top of bed from the outcrop between Klubina and Zborov nad Bystricou villages. **D** — Detailed view from the Krásno nad Kysucou outcrop showing clustered amalgamation clasts. **E** — Detailed view from the quarry between Klubina and Zborov nad Bystricou villages showing post-sedimentary deformation of claystone/silty claystone with mm to cm silt/very fine sandstone laminae. **F** — Detailed view from the Krásno nad Kysucou outcrop showing submarine slump. **G** — General view of the quarry between Klubina and Zborov nad Bystricou villages. **H** — Detailed view from the outcrop in Lysá pod Makytou quarry showing imprints of shale clasts at the top of a sandstone bed. **I** — General view of a part of the quarry near Veľké Rovné village. **J** — Detailed view from the quarry between Klubina and Zborov nad Bystricou villages showing imprint of shale clasts at the top of sandstone beds. **K** — Detailed view from the quarry between Klubina and Zborov nad Bystricou villages showing claystone/silty claystone with mm to cm silt/very fine sandstone laminae (Facies A7).

of observed transitions of facies. The matrix of significant facies transitions summarizes the possibilities of non-random facies transitions, calculated at a significance level of 0.5 and expressed by the number of percent.

The vertical arrangement of different facies can be presented by a variety of facies relationship diagrams. Their aim is to present either the raw data or statistics based on those data in a format which aids interpretation (Graham 1988). Non-random facies transitions were presented by the scheme of significant facies transitions. This scheme was compared to the facies successions in deep-water facies models allowing the interpretation of depositional processes.

Results

Significant facies transitions

There were eight descriptive lithofacies A1, A2, ..., A8 (Table 1), distinguished in the studied sedimentary succes-

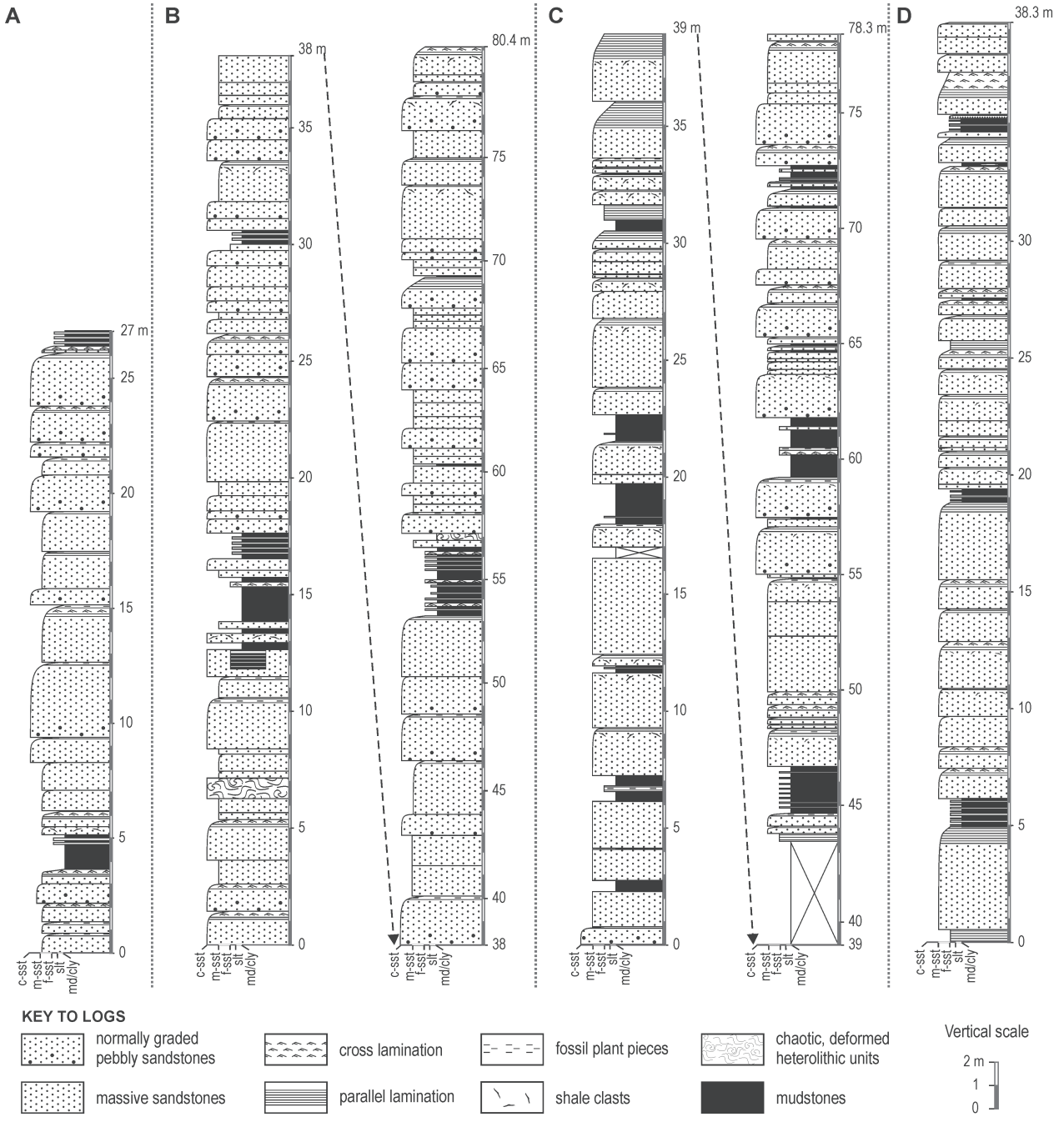

Fig. 3. Sedimentary logs of representative parts of studied sedimentary sequences of the Kýčera Member from: **A** — the quarry near Lysá pod Makytou village. **B** — the quarry near Veľké Rovné village. **C** — the quarry between Klubina and Zborov nad Bystricou villages. **D** — the road-cut near Krásno nad Kysucou village. See the outcrop locations on Fig. 1A.

Table 1: Lithofacies.

Facies Code	Mean Thickness (cm)	Description
A1	77	structureless (massive) sandstone
A2	118	pebbly sandstone with normally graded pebbles
A3	21	parallel laminated sandstone
A4	9	rippled, wavy laminated very fine sandstone to siltstone
A5	7	laminated, very fine sandstone to siltstone
A6	47	mudstone
A7	78	claystone/silty claystone with mm to cm silt/very fine sandstone laminae
A8	262	chaotic, deformed heterolithic units

sions (Fig. 3) during the field research, tested for ordered arrangement using the computer calculation of Markov Chains. The facies transitions A1–A3, A1–A5, A1–A7, A1–A8, A2–A3, A2–A5, A3–A4, A4–A5, A5–A1, A5–A2, A5–A6, A5–A7, A6–A1, A6–A2, A6–A8, A7–A1, A7–A2 reached the probability higher than 95 %, that is they are non-random with the probability higher than 95 % (Table 3). These transitons were considered regular at significance level of α=0.5. All of these significant facies transitions are illustrated in the scheme of significant facies transitions (Fig. 4).

Discussion

Analysis of facies and flow dynamics

In the interpretation of significant facies transitions it is important to keep in mind that the calculated significant transitions represent the most probable facies transitions, but not their frequency in the studied sedimentary sequences. The real frequencies of facies transitions are written down in the matrix of observed facies transitions (Table 2). There-

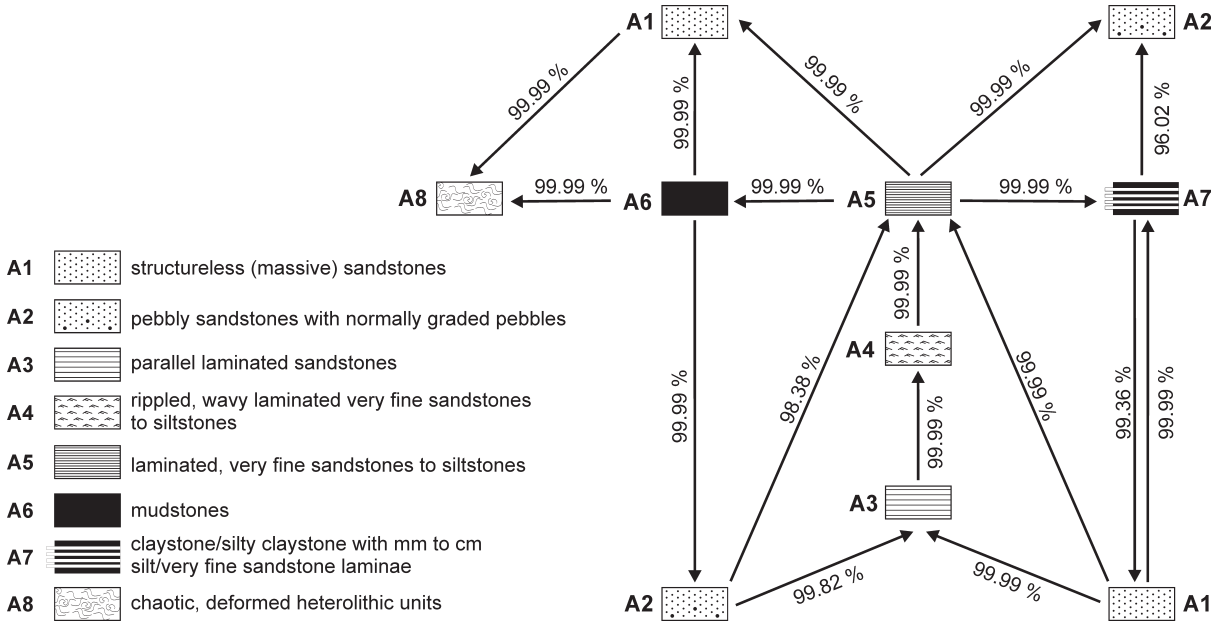

Fig. 4. Scheme of significant facies transitions. Facies codes are described in Table 1.

Table 2: Matrix of observed facies transitions.

Facies	A1	A2	A3	A4	A5	A6	A7	A8	Sum of row
A1	–	19	65	0	160	60	12	2	318
A2	18	–	13	0	33	14	0	0	78
A3	5	0	–	74	1	1	0	0	81
A4	5	3	0	–	65	12	0	0	85
A5	144	24	0	5	–	97	6	0	276
A6	126	27	2	6	25	–	3	1	190
A7	14	4	1	0	0	3	–	0	22
A8	1	0	0	0	1	1	0	–	3
Sum of column	313	77	81	85	285	188	21	3	

Table 3: Matrix of significant facies transitions.

Facies	A1	A2	A3	A4	A5	A6	A7	A8
A1	–	–	99.99	–	99.99	–	99.99	99.99
A2	–	–	99.82	–	98.38	52.02	–	–
A3	–	–	–	99.99	–	–	–	–
A4	–	–	–	–	99.99	–	–	–
A5	99.99	99.99	–	–	–	99.99	99.99	–
A6	99.99	99.99	–	–	–	–	–	99.99
A7	99.36	96.02	–	–	–	–	–	–
A8	–	–	–	–	36.46	58.74	–	–

fore, when interpreting sedimentary successions it is useful to consider both statistically significant and real facies transitions in order to better understand their significance and real occurrence in the studied sedimentary record.

The calculated significant successions of facies A1–A3–A4–A5–A6 and A2–A3–A4–A5–A6 (Fig. 4) remarkably resemble a Bouma sequence (Bouma 1962). This succession of lithofacies is considered a typical sequence deposited by turbidity currents. It comprises a massive or graded sandstone interval T_a (facies A1 or A2) at the base, followed upwards by laminated sandstone interval T_b (facies A3), then passing to a rippled/wavy interval T_c (equivalent to A4 facies), upper laminated siltstone interval T_d (facies A5) and terminating with mud interval T_e (facies A6). The real occurrence of this succession of facies in the sedimentary record (Fig. 2A,B) was considered with reference to the matrix of observed facies transitions (Table 2). There are 396 A1/A2–AX facies transitions in the matrix of observed facies transitions, but only 78 of them (= 19.70 %) are A1/A2–A3 transitions resembling T_{a-b} intervals of the Bouma sequence (Fig. 2B). There are also 74 A3–A4 facies transitions (equivalent to T_{b-c} Bouma intervals), 65 A4–A5 facies transitions (equivalent to T_{c-d} Bouma intervals) and 97 A5–A6 facies transitions (equivalent to T_{d-e} Bouma intervals) in the matrix of observed facies transitions (Table 2). This means that only 19.70 % of the sandy intervals beginning with the A1 or A2 facies constitute either a complete or a basal part of the classical Bouma sequence. In addition to A1/A2–A3 facies transitions, the A1 or A2 facies can also be followed by the A5, A6, A7, A8 facies as well as by the A1 or A2 facies. The A1 or A2 facies are most frequently followed by facies A5. There are 193 transitions of A1/A2–A5 facies in the matrix of observed facies transitions (Table 2). It is 48.74 % of the whole 396 transitions of A1/A2–AX facies in the matrix of observed facies transitions. While the previously discussed transitions of facies A1/A2–A3 can be compared to the T_{ab} Bouma divisions, the A1/A2–A5 transitions resemble rather the T_{ad} Bouma divisions. According to the field record, the units of facies A5 are usually much thinner than those of the A1 or A2 facies. This may suggests that apart from the deposits of turbidity currents (Bouma sequence), perhaps the most significant part of the massive or graded sandstone beds with thin, fine laminated tops in the investigated sections are products of probably the most disscussed deep-water sediment gravity flows, frequently interpreted as high-density turbidity currents (Lowe 1982), concentrated density flows (comp. Mulder & Alexander 2001) or sandy debris flows (Shanmugam 1997), while their upper laminated tops were deposited from dilute current. These tops contain pieces of mica and fossil plants and they are frequently bioturbated (Fig. 2C). They could be reworked by bottom currents. The A1/A2–A6 facies transitions have a similar explanation. At the top of the A1 or A2 facies there are sometimes shale clasts. They apparently represent rip-down clasts (Fig. 2H,J) that indicate post-depositional liquefaction (Stow & Johansson 2000). Sometimes, amalgamated intervals in the investigated sedimentary section are indicated by the presence of clustered amalgamation clasts (Fig. 2D) formed by erosional break-up of a thin intervening shale layer between successive sand deposits (see Stow & Johansson 2000).

Facies A7 most probably follows the A1 or A5 facies (Fig. 2K). Facies A7 is considered to represent repetitive A5–A6 facies transitions and it is interpreted as representing deposition from low-concentration turbidity currents. According to the matrix of observed facies transitions (Table 2), the facies A6 follows all the defined facies. It is most likely to follow A2, A5 or A8 facies (Table 3). Thick intervals of A6 facies were deposited from suspension fallout. Facies A8 represents chaotic, contorted heterolithic units, which commonly overlie A1 or A6 facies (Table 3, Fig. 4). The A8 facies is apparently formed by submarine slumps (Fig. 2F). In some cases, they could be the result of post-sedimentary deformation (Fig. 2E).

Genetic facies definition

The examination of both the calculated significant facies transitions and the original sedimentary records allowed us to define six genetic facies types, which were compared to the standard deep-water facies models and schemes of deep-water gravity-driven deposits. The genetic facies, when arranged laterally according to the declining grain size, provide the evidence of deposition from increasingly diluted and more mature flows (Fig. 5). Such facies arrangement reflects depositional settings from proximal to distal. The most proximal and usually the coarsest facies are chaotic and deformed units (Facies no. 1 in Fig. 5), which apparently developed on the slope of depositional lobes. However, some of these units may developed as post-sedimentary deformations. The next facies represent thick- to medium-bedded sandstones with normally graded granules and pebbles (Facies no. 2 in Fig. 5) and thick- to medium-bedded structureless sandstones (Facies no. 3 in Fig. 5). These facies reflect the deposits of density flows (Alexander & Mulder 2001) or dense flows (sensu Mutti et al. 2003) or high-concentration turbidity currents (Lowe 1982; Pickering et al. 1986). Both these facies types may have thin laminated tops, which developed as the flows were progressively diluted by the entrainment of surrounding water. Normal gradation developed if the dilution of water was sufficient to allow particle fall out within the flow. The next facies (Facies no. 4 in Fig. 5) are characterized by the Bouma sequence of structures, representing deposits from turbidity currents. The next facies (Facies no. 5 in Fig. 5) are claystone/silty claystone with mm to cm silt to very fine sandstone laminae. These facies are compared to the deposits of low-concentration turbidity currents. The last and the most distal facies are claystones or

Genetic facies identification				
Facies code	Selected non-random facies transitions	Facies description	Dominant particle support and depositional mechanisms	Facies codes of other writers*
1	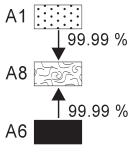	chaotic, deformed heterolithic units	syn- and post- depositional deformation	P: F
2 a,b	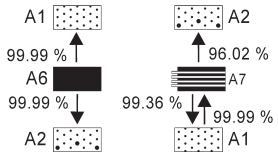	thick- to medium-bedded coarse to medium sandstone with dispersed, normally graded granules and pebbles near the base (usually less than 20 %), subtype b — have thin, parallel laminated siltstone cap that usually constitute less than 5 % of the bed thickness	high-concentration turbidites, dense flows (Mutti et al. 2003) subtype a: hyperconcentrated, subtype b: concentrated dense flows (Mulder & Alexander 2001)	P: A2.7, ?B M: F5 M&L: ?A1, C1
3 a,b	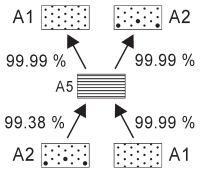	medium to thick-bedded structureless medium to fine sandstone and muddy sandstone, subtype a — sharp bounding surface, subtype b — have thin, parallel laminated siltstone cap at the top that usually constitute less than 5 % of the bed thickness	dense flow - turbulent flow: possibly residual flow originating during the dense flow transformation into turbulent flow (see Mutti et al. 2003)	P: B1.1, C1.1 M: ?F5, F8 M&L: ?C1
4 a,b	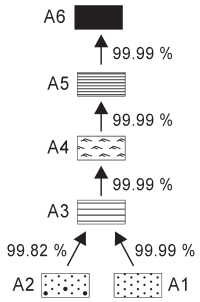	medium- thick-bedded sandstone and muddy sandstone with structures internally organized into Bouma intervals; subtype a — starts with A1 lithofacies, subtype b — starts with A2 lithofacies	turbulent flow (Mutti et al. 2003) sandy debris flow at the base + turbidity flow at the top (Shanmugam 1997)	P: C2.1, C2.2 M: F8 + ?F9 M&L: ?C1, C2
5	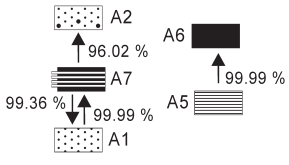	claystone/silty claystone with mm to cm silt — very fine sandstone laminae, massive to parallel laminated and starved ripple laminated	low-concentration turbidity currents and suspension fallout	P: D2, E M&L: D, E
6	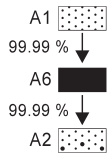	claystone or silty claystone, massive or parallel laminated	suspension fallout, low-concentration turbidity currents	P: E2 M&L: G

** P: — Pickering et al. (1989, 1986); M: — Mutti et al. (2003); M&L: — Mutti & Ricci Lucchi (1972)*

Fig. 5. List of genetic facies with their characterization compared to some deep-water facies models.

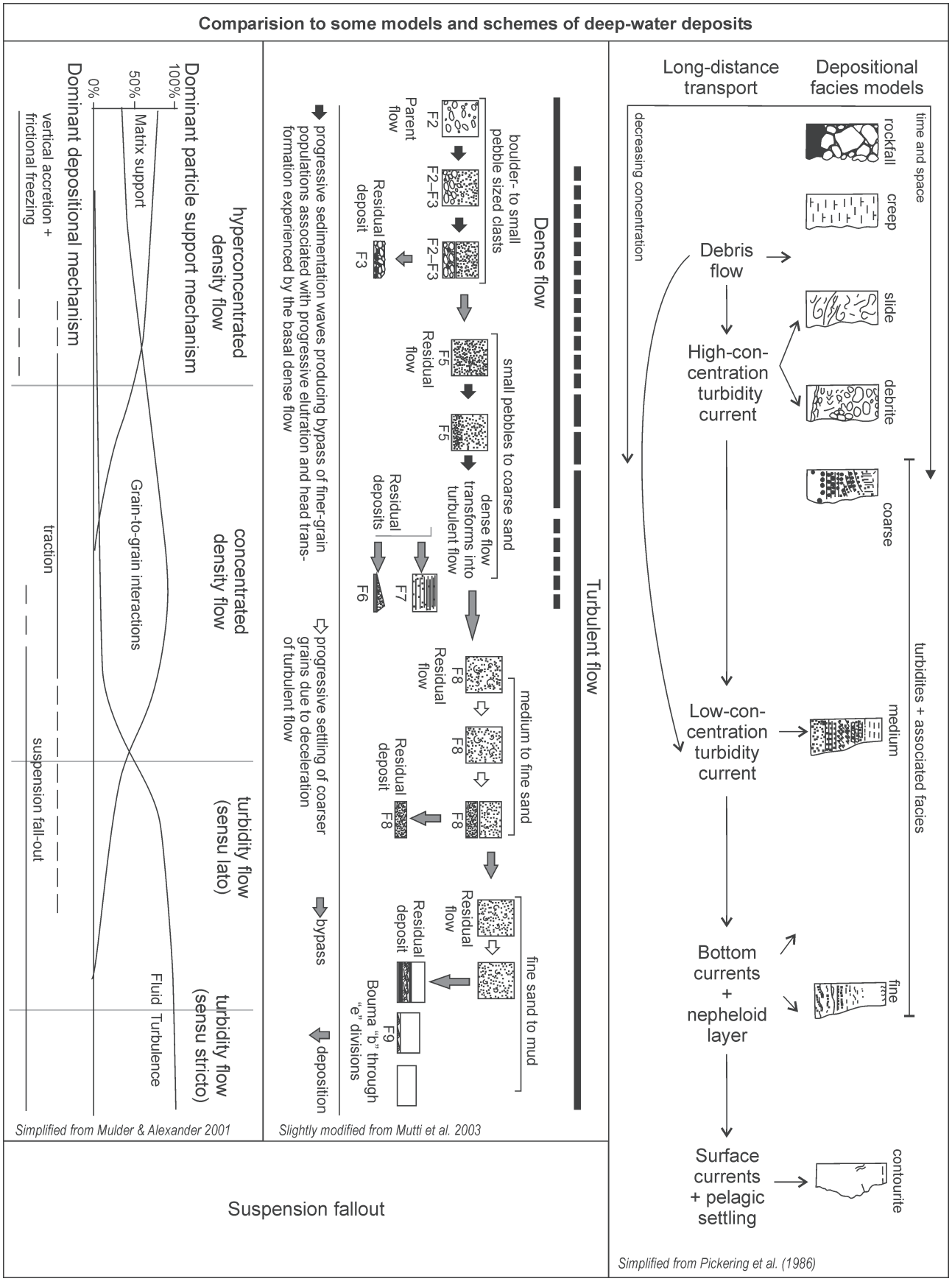

Fig. 5. *Continued.*

silty claystones (Facies no. 6 in Fig. 5), which are compared to the deposits of low-concentration turbidity currents or suspension fallout.

Conclusions

The application of Markov Chain analysis allowed us to identify ordered succession of descriptive facies or structures in a turbiditic formation from the Magura Zone of the Outer Western Carpathians. Significant facies transitions were determined providing the evidence that classical turbidites constitute the important part of the studied sedimentary sequences of the Kýčera Member. In addition to turbidite currents, the Kýčera Member facies were also deposited by density flows, suspension fallout or they were reworked by bottom currents or resulted from syn- or post-depositional deformation.

In this paper, the Markov Chain analysis has been applied to calculate the arrangement of facies in turbiditic formation, although it has been utilized in the past for the analysis of ordered sequences of facies in other environments (e.g. meandering river, shallow-marine, beach-barrier etc.). The calculation aspects of Markov analysis are reviewed in a concise and instructive form, therefore this study can serve as a case study for the application of the Markov Chains in the interpretations of sedimentary sequences in the field or from boreholes. A subsequent contribution of this study was the creation of a self-designed computer program, named phpSedistat. Computer-based calculation of regular facies transitions noticeably simplified and hastened the utilization of Markov Chains.

Acknowledgments: This study was supported by the Slovak Research and Development Agency (APVV 51-011305 Project) and by VEGA Grant GA 6093. Official reviews by Prof. Dr. Nestor Oszczypko, Dr. Ivan Baráth and Prof. Dr. Szczepan Porębski provided insightful comments that helped improve the original manuscript.

References

Biely A. (Ed.), Bezák V., Elečko M., Gross P., Kaličiak M., Konečný V., Lexa J., Mello J., Nemčok J., Potfaj M., Rakús M., Vass D., Vozár J. & Vozárová A. 1996: Geological map of Slovakia, 1:500,000. *Ministry of Environment SR & State Geological Institute of Dionýz Štúr*, Bratislava.

Bombita G. & Pop G. 1991: Mesozoic formations from Poiana Botizii, Pieniny Klippen Belt of Romania. *Geol. Carpathica* 42, 3, 139–146.

Bouma A.H. 1962: Sedimentology of some flysch deposits. *Elsevier*, Amsterdam, 1–168.

Carr T.R. 1982: Log-linear models, Markov chains and cyclic sedimentation. *J. Sed. Petrology* 52, 905–912.

Dasgupta P. 2003: Sediment gravity flow — the conceptual problems. *Earth Sci. Rev.* 62, 265–281.

Doveton J.H. 1971: An application of Markov Chain analysis to the Ayrshire Coal Measures succession. *Scott. J. Geol.* 7, 11–27.

Eliáš M., Schnabel W. & Stráník Z. 1990: Comparison of the Flysch Zone of the Eastern Alps and the Western Carpathians based on recent observations. In: Minaříková D. & Lobitzer H. (Eds.): Thirty years of geological cooperation between Austria and Czechoslovakia. *Geol. Surv.*, Praha, 37–46.

Ethier V.G. 1975: Application of Markov analysis to the Banff Formation (Mississippian), Alberta. *Math. Geol.* 7, 47–61.

Gingerich P.D. 1969: Markov analysis of cyclic alluvial sediments. *J. Sed. Petrology* 39, 330–332.

Goodman L.A. 1968: The analysis of cross-classified data: independence, quasi-independence and interactions in contingency tables with or without missing entries. *J. Amer. Statist. Assoc.* 63, 1091–1131.

Graham J. 1988: Collection and analysis of field data. In: Tucker M. (Ed.): Techniques in sedimentology. *Blackwell Sci. Publ.*, 1–394.

Harper C.W. Jr. 1984: Improved methods of facies sequence analysis. In: Walker R.G. (Ed.): Facies models. *Geosci. Can Reprint* 1, 11–13.

Lowe D.R. 1982: Sediment gravity flows: II. Depositional models with special reference to the deposits of high-density turbidity currents. *J. Sed. Petrology* 52, 279–297.

Miall A.D. 1973: Markov Chain analysis applied to an ancient alluvial plain succession. *Sedimentology* 20, 347–364.

Mulder T. & Alexander J. 2001: The physical character of subaqueous sedimentary density flows and their deposits. *Sedimentology* 48, 269–299.

Mutti E. 1992: Turbidite sandstones. *Inst. Geol. Univ. Parma,* 1–275.

Mutti E. & Ricci Lucchi F. (1972): Le torbiditti dell'Appenino settrentrinale, introduzione all´analisi di facies. *Soc. Geol. Ital., Mem.* 11, 161–199.

Mutti E., Tinterri R., Benevelli G., di Biase D. & Cavanna G. 2003: Deltaic, mixed and turbiditic sedimentation of ancient foreland basins. *Mar. Petroleum Geol.* 20, 733–755.

Oszczypko N. 1992: Late Cretaceous through Paleogene evolution of Magura basin. *Geol. Carpathica* 43, 6, 333–338.

Oszczypko N., Golonka J., Malata T., Poprawa P., Słomka T. & Uchman A. 2003: Tectono-stratigraphic evolution of the Outer Carpathian basins (Western Carpathians, Poland). *XVIIth Congress of the Carpathian-Balkan Geological Association, Bratislava, Post-Congress Proceedings. Miner. Slovaca* 35, 17–20.

Pickering K., Stow D., Watson M. & Hiscott R. 1986: Deep-water facies, processes and models: a review and classification scheme for modern and ancient sediments. *Earth Sci. Rev.* 23, 75–174.

Plašienka D., Grecula P., Putiš M., Kováč M. & Hovorka D. 1997: Evolution and structure of the Western Carpathians: an overview. In: Grecula P., Hovorka D. & Putiš M. (Eds.): Geological evolution of the Western Carpathians. *Miner. Slovaca — Monogr.*, Bratislava, 1–24.

Potter P.E. & Blakey R.F. 1968: Random processes and lithologic transitions. *J. Geol.* 76, 154–170.

Powers D.W. & Easterling R.G. 1982: Improved methodology for using embedded Markov chains to describe cyclical sediments. *J. Sed. Petrology* 52, 913–923.

Read W.A. 1969: Analysis and simulation of Namurian rocks of Central Scotland using a Markov-process model. *Math. Geol.* 1, 199–219.

Schwarzacher W. 1975: Sedimentation models and quantitative stratigraphy. *Elsevier*, Amsterdam, 1–382.

Shanmugam G. 1997: The Bouma sequence and the turbidite mind set. *Earth Sci. Rev.* 42, 201–229.

Shanmugam G. 2002: Ten turbidite myths. *Earth Sci. Rev.* 58, 311–341.

Stow D.A.V. 2005: Sedimentary rocks in the field. A colour quide. *Manson Publ.*, London, 1–320.

Stow D.A.V. & Johansson M. 2000: Deep-water massive sands: nature, origin and hydrocarbon implications. *Mar. Petrol. Geol.* 17, 145–174.

Weedon G.P. 2005: Time-series analysis and cyclostratigraphy: Examining stratigraphic records of environmental cycles. *Cambridge University Press*, 1–273.

Wilkinson B.H., Drummond C.N., Rothman E.D. & Diedrich N.W. 1997: Stratal order in peritidal carbonate sequences. *J. Sed. Res.* 67, 1068–1082.

Żytko K., Zając R., Gucik S., Ryłko W., Oszczypko N., Garlicka I., Nemčok J., Eliáš M., Menčík E. & Stráník Z. 1989: Map of the tectonic elements of the Western Outer Carpathians and their Foreland. In: Poprawa D. & Nemčok J. (Eds.): Geological atlas of the Western Outer Carpathians and their foreland. *PIG Warszawa/GÚDŠ Bratislava/ÚÚG Praha*.

Appendix

Step-by-step list of procedures incorporated into the phpSedistat program:

1. The matrix of observed facies transitions is created.

As the quasi-independence principle was applied (see e.g. Carr 1982; Powers & Easterling 1982 for details), the facies transitions between the same facies were excluded. They are usually hardly identified in the field.

2. The matrix of random transitions is calculated.

Row/column sums of the matrix of observed facies transitions and parameters a_i, b_j are utilized to calculate the matrix of random transitions. Parameters a_i, b_j are estimated using an iterative solution (see Powers & Easterling 1982).

The first iteration of a_i and b_j is calculated as follows:

$$a_i^{(1)} = \frac{n_{i+}}{(m-1)}, \qquad i = 1, 2, ..., m \tag{1}$$

$$b_j^{(1)} = \frac{n_{+j}}{\sum_{i \neq j} a_i^{(1)}}, \qquad j = 1, 2, ..., m \tag{2}$$

where m is a number of facies members, n_{i+} is an i^{th} row sum and n_{+j} is a sum of j^{th} column.

Then the i^{th} iteration is calculated as follows (3, 4):

$$a_i^{(I)} = \frac{n_{i+}}{\sum_{j \neq 1} b_j^{(I-1)}}, \qquad i = 1, 2, ..., m \tag{3}$$

$$b_j^{(I)} = \frac{n_{+j}}{\sum_{i \neq j} a_i^{(I)}}, \qquad j = 1, 2, ..., m \tag{4}$$

The iteration is continued until (5, 6):

$$|a_i^{(I)} - a_j^{(I-1)}| < 0.01\, a_i^{(I)}, \quad \text{for } i = 1, ..., m \tag{5}$$

and

$$|b_j^{(I)} - b_j^{(I-1)}| < 0.01\, b_j^{(I)}, \quad \text{for } j = 1, ..., m \tag{6}$$

Let a' and b' be the last iterations of $a_i^{(I)}$ and $b_j^{(I)}$, then the estimated random transitional frequencies are calculated as follows (7):

$$E_{ij} = a_i' \cdot b_i' \qquad i = 1, 2, ..., m;\ j = 1, 2, ..., m;\ i \neq j \tag{7}$$

3. The matrix of observed possibilities of facies transitions and the matrix of random possibilities of facies transitions are calculated.

The matrix of observed transition frequencies and the matrix of random transition frequencies are recalculated through their row sums, e.g. the first row is recalculated as follows:

$$a_{12}/n_{1+},\ a_{13}/n_{1+},\ ...\ a_{1m}/n_{1+} \tag{8}$$

The result of these recalculations is the creation of the matrix of observed possibilities of facies transitions and the matrix of random possibilities of facies transitions.

4. Calculation of a difference matrix.

The difference matrix is calculated as the matrix of random possibilities of facies transitions is substracted from the matrix of observed possibilities of facies transitions.

5. Positive values in a difference matrix are tested.

All positive values in the difference matrix are tested for randomness at a selected significance level. Testing procedures within the phpSedistat computer program are provided at significance level 0.5. It means that all computed values greater than 0.05 are non-random with the possibility less than 5 %, i.e. random with the possibility greater than 95 % and all computed values less than 0.05 are non-random with the possibility greater than 5 %. The testing criterion is as follows (see Harper 1984):

$$\sum_{n=n_{cont}}^{n=N} \frac{N!}{(N-n)!n!} \cdot p^n \cdot q^{N-n} \tag{9}$$

where N = relevant row sum in the matrix of observed transition frequencies, n_{cont} = observed number of a specific transition, p = the possibility of a specific transition in the matrix of random possibilities of transition frequencies and q = 1–p.

6. The matrix of regular facies transitions is created.

The values computed in the testing procedure are multiplied by 100 and the matrix of regular facies transitions is created, where the regular facies transitions are calculated at the significance level 0.5 and expressed in the number of percent. The formulation of the resulting possibilities of facies transition in the number of percent simplifies their evaluation.

The program phpSediStat was programmed under a GNU lincence as an open source software product. It can be downloaded from http://phpsedistat.sourceforge.net.